Supporting Information

Triisopropylsilylethynyl-Substituted Solid Additives for Morphology Optimization Enabling High-Efficiency Organic Solar Cells

Siyuan Zang[a,#], Jia Wang [b,#], Shuaiqi Wang[a], Wenying Zhou[b], Hongxiang Li[c,d*], Bin Kan[b], Qian Zhang[a,*]

a. Key Laboratory of Organosilicon Chemistry and Material Technology, Ministry of Education, Zhejiang Key Laboratory of Organosilicon Material Technology, College of Material, Chemistry and Chemical Engineering, Hangzhou Normal University, Hangzhou 311121, China. E-mail: qzhang@hznu.edu.cn.

b. School of Materials Science and Engineering, National Institute for Adv. Mater., Nankai University, Tianjin 300350, China.

c. College of Materials and Energy, Guang'an Institute of Technology, Guang'an 638000, China. Email: lihongxiang@scu.edu.cn.

d. College of Polymer Science and Engineering, National Key Laboratory of Advanced Polymer Materials, Sichuan University, Chengdu 610065, China.

[#]Zang S and Wang J contributed equally to this work.

1. Materials

Polymer donor PM6 and small molecular acceptor L8-BO were purchased from Hyper Inc., and 2PACz was purchased from TCI Chemical Co. All the other reagents and chemicals were purchased from commercial suppliers and were used directly without further purification unless otherwise noted.

2. Measurements and Instruments

^{1}H-NMR and ^{13}C-NMR spectra were recorded on a Bruker AVANCE 500 spectrometer. ^{1}H NMR and ^{13}C NMR spectra were referenced to tetramethylsilane (0 ppm) for $CDCl_3$.

Thermal gravimetric analyses (TGA). TGA measurements were performed on TA Q500 instrument under nitrogen gas flow with a 10 ^{o}C min^{-1} heating rate from room temperature to 300 ^{o}C. **Differential scanning calorimetry (DSC).** DSC measurements were performed on a TG209 DSC204 DMA242 METTLER3+ DSC instrument with a heating rate of 10 ^{o}C min^{-1} under a nitrogen atmosphere, with a temperature range from room temperature to 120 ^{o}C.

Molecular dynamic (MD) method. All molecular dynamics simulations were conducted utilizing the GROMACS (2023.3) software package[1], employing the GROMOS force field. The restrained electrostatic potential (RESP) fitting technique was applied to derive partial charges for each molecule. For D18/L8-BO with Ph-BTBT-10 blend film, 44 D18 molecules with 3 repeat units and 216 L8-BO molecules were randomly put in the box of 30 × 30 × 30 nm^3, and then 65 Ph-BTBT-10 were inserted. All these ratios are consistent with the experimental ratios. All these BHJs films were annealed from 500 K down to 450 K gradually, during 100 ns. The production run lasted 100 ns after an equilibration run of 50 ns. The box sizes, densities and energy analysis were analyzed from the production run. The LINCS algorithm[2] was utilized to constrain covalent bonds involving hydrogen atoms. A simulation time step of 1.0 femtoseconds was employed. Both the pressure and temperature were regulated using the Parrinello–Rahman barostat at 1 atm and the Nose–Hoover thermostat[3, 4], respectively. The graphics were processed by the Visual Molecular Dynamics (VMD)

program[5].

Density Functional Theory (DFT) Calculations. All alkyl chains were replaced with methyl groups (-CH_3) to reduce the computational requirements. The ground-state geometry structures were optimized by density functional theory (DFT) under the Becke three-parameter Lee-Yang-Parr (B3LYP) functional combining with 631G(d) the vibrational frequencies were calculated after geometries optimization and no imaginary frequency was found. All the DFT calculations were performed in the Gaussian 16 package.

UV-visible (UV-vis) absorption. UV-vis absorption spectra and variable-temperature UV-vis absorption spectra were recorded on a Cary 5000 UV-vis spectrophotometer.

Atomic force microscopy (AFM). The AFM images were obtained from a Bruker Dimension Icon atomic force microscope by using in tapping mode. The film samples were prepared under the same conditions as those used for device fabrication.

Transient photocurrent/photovoltage (TPC/TPV). The TPC/TPV were performed on a Molex 180081-4320 with a light intensity of about 0.5 sun. Current dynamics was recorded on a digital oscilloscope (Tektronix MDO4104C), and currents under short circuit conditions was measured over a 50 Ω resistor. The optimized devices were used for TPC measurements directly.

Measurement of charge carrier mobility. The hole and electron mobility were measured by using space-charge-limited (SCLC) method. Hole mobility was measured with the device structure of ITO/PEDOT:PSS/active layer/MoO_3/Ag. Electron mobility was measured with the device structure of ITO/ZnO/active layer/PNDIT-F3N/Ag. The hole and electron mobility estimated by the following equation: $J=9\varepsilon_0\varepsilon_r\mu V^2/8d^3$, where J is the current density, ε_0 is the vacuum permittivity, ε_r is the relative dielectric constant, V is the internal voltage in the device, and d is the thickness of the active layer.

GIWAXS and GISAXS Measurement. GIWAXS data were obtained at beamline BL02U2 of Shanghai Synchrotron Radiation Facility (SSRF). The monochromatic of the light source was 1.24 Å. The data were recorded by using the two-dimensional

image plate detector of Pilatus 2M from Dectris, Switzerland.

The incidence angle was 0.2°, and the sample-to-detector distance was 2200 mm by calibration for GISAXS.

The GISAXS 1D profiles were fitted with a universal model following Equation (1). Data fitting was done using Sas View (version 5.01) software.

$$I(q) = \frac{A_1}{[1 + (q\xi)^2]^2} + A_2 \langle P(q,R) \rangle S(q, R, \eta, D) + B \tag{1}$$

$$S(q) = 1 + \frac{sin[(D-1)tan^{-1}(q\eta)]b \pm \sqrt{b^2 - 4ac}}{(qR)^D} \frac{D\Gamma(D-1)}{[1 + \frac{1}{(q\eta)^2}]^{(D-1)/2}} \tag{2}$$

where A_1, A_2, and B are independent fitting parameters and q is the scattering wave vector. The average correlation length ξ of the PM6 domain and the Debye-Andersone-Brumberger (DAB) term make up the first term. The contribution from L8-BO fractal-like aggregations is seen by the second term. Here, R is the mean spherical radius of the primary L8-BO particles, P (q, R) is the form factor of the L8-BO, S (q, *R*, *η*, *D*) is the fractal structure factor to explain the primary particles interaction in this fractal-like aggregation system, *η* is the correlation length of the fractal-like structure, and *D* is the fractal dimension of the network. Equation 3 was used to calculate the average domain size by the Guinier radius of the fractal like network R_g. 2Rg (the product of *η* and *D*) is regarded as the domain size of acceptor aggregation.

$$R_g = \eta \sqrt{\frac{D(D+1)}{2}} \tag{3}$$

Miscibility measurement: Contact angle measurements were carried out by an Kruss DSA100, using water and glycerin by sessile drop analysis. The surface tension values of films are calculated by[6]:

$$\gamma_{wat}(cos\theta_{wat} + 1) = 2\sqrt{\gamma_{wat}^d \gamma^d} + 2\sqrt{\gamma_{wat}^p \gamma^p}$$

$$\gamma_{MI}(cos\theta_{Gly} + 1) = 2\sqrt{\gamma_{Gly}^d \gamma^d} + 2\sqrt{\gamma_{Gly}^p \gamma^p}$$

$$\gamma = \gamma^d + \gamma^p$$

where θ is the contact angle of each thin film, and γ is the surface tension of samples, which is equal to the sum of the dispersion (γ^d) and polarity (γ^p) components; γ_{wat} and γ_{Gly} are the surface tensions of the water and glycerin; and γ_{wat}^{d}, γ_{wat}^{p}, γ_{Gly}^{d} and γ_{Gly}^{p} are the dispersion and polarity components of γ_{wat} and γ_{Gly}. The Flory-Huggins interaction parameters are deduced from: $\chi_{D\text{-}A} = k(\sqrt{\gamma_D}-\sqrt{\gamma_A})^2$, where k is a positive constant at a specific temperature[7].

3. Device Fabrication and Characterization

The OSCs were fabricated with a conventional structure of ITO/2PACz/Active layer/PNDIT-F3N/Ag. In detail, ITO coated glass substrates were cleaned in turn with detergent water, deionized water, acetone and isopropyl alcohol in an ultrasonic bath sequentially for 15 mins and dried by nitrogen purge. Before use, the surface of ITO-coated glass was treated in an ultraviolet-ozone chamber for 20 min. Then a thin layer of [2-(9H-Carbazol-9-yl)ethyl]phosphonic acid (2PACz) (dissolved in ethanol at the concentration of 0.3 mg mL^{-1}) was first spin-coated on the ITO substrates with 3000 rpm for 20 s. Subsequently, the 2PCAz films were baked at 100°C for 10 mins under ambient conditions and transferred to a glovebox filled with nitrogen. The PM6:L8-BO (1:1.2, w/w) were dissolved in chloroform at the donor concentration of 7 mg/mL with 50 wt% and 20 wt% 2T-Si and TT-Si, respectively. And the ternary device based on PM6:L8-BO:BTP-eC9 (1:0.8:0.4) was dissolved in chloroform at the donor concentration of 7 mg/mL with 50 wt% 2T-Si. All the solutions need to be stirred at room temperature for 4 hours, and were spin-casted at 2000 rpm for 30 s onto the 2PACz layer. After spin-coating, the blend films were annealed at 90°C for 5 mins. After cooled down, the methanol solution of PNDIT-F3N (1 mg/mL) was spin-coated on the top of the active layer at 3000 rpm for 20 s. Finally, Ag electrode with the thickness of 150 nm was evaporated under 2×10^{-6} Pa. The active area of the device was 4 mm^2, and a shadow mask with an area was about 3.24 mm^2 in our laboratory. The glue dispenser/spin coater (Brand-REESEEN, PvS-mini7) used in the lab are from Jiangyin J. Wanjia Technology Co., Ltd.

The current density-voltage (*J-V*) curves of OSCs were recorded on a Keithley 2400 source-measure unit in a glove box filled with nitrogen. Enli SS-F5-3A solar

simulator with AM1.5 G was used as the light source, and the light intensity was 100 mW cm^{-2} which was calibrated by a standard Si solar cell (made by Enli Technology Co., Ltd., Taiwan, and calibrated report can be traced to NREL). A QE-R Solar Cell Spectral Response Measurement System was used to measure the external quantum efficiency (EQE) values of the devices. A Veeco Dektak 150 profilometer was used to measure the thickness of the active layers.

4. Synthesis

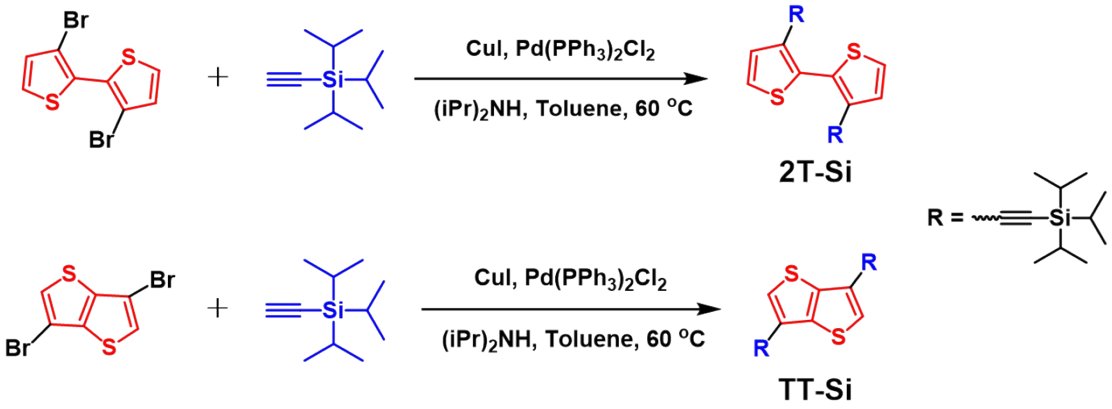

Scheme S1. Synthetic route of the solid additives 2T-Si and TT-Si.

3,3'-Bis(triisopropylsilylethynyl)-2,2'-dithiophene (2T-Si): 3,3′-Dibromo-2,2′-bithiophene (500 mg, 1.543 mmol) was dissolved in THF (25 mL) and diisopropylamine (25 mL) in a two-neck round-bottom flask that is adapted with a reflux condenser. Under N_2 atmosphere, CuI (29 mg, 0.154 mmol), $(PPh_3)_2PdCl_2$ (54 mg, 0.0771 mmol), and triisopropylsilylacetylene (704 mg, 3.857 mmol) were then added. The mixture was stirred at 60 °C for 6 hours. Then the reaction mixture was cooled to room temperature, and poured into water (150 mL) and extracted with dichloromethane (100 mL × 3). The combined organic extracts were dried over anhydrous $MgSO_4$. After concentrate the organic layer by vacuum evaporation, the raw product was purified with chromatography column by using petroleum ether as the eluent. 2T-Si was obtained as a white solid (675 mg, 1.281 mol, 83%). ^{1}H NMR (500MHz, $CDCl_3$) δ: 7.16 (d, *J* = 5.25 Hz, 2H), 7.07 (d, *J* = 5.25 Hz, 2H), 1.14-1.11 (m, 42H). ^{13}C NMR (126 MHz, $CDCl_3$): δ 138.83, 127.52, 90.19, 81.60, 18.71, 18.57, 11.42,11.32.

3,6-Bis(triisopropylsilylethynyl)thieno[3,2-*b*]thiophene (TT-Si): TT-Si (698 mg,

1.393 mol, 81%**)** was obtained as a white solid from 3,6-dibromothieno[3,2-*b*]thiophene (500 mg, 1.67 8mmol), triisopropylacetylene (765 mg, 4.195 mmol), $(PPh_3)_2PdCl_2$ (59 mg, 0.0839 mmol) and CuI (32 mg, 0.168 mmol), using anhydrous diisopropylamine/THF (25 mL/25 mL) as the solvent, following the procedure for the synthesis of 2T-Si. ^{1}H NMR (500MHz, $CDCl_3$) δ: 7.33 (s, 2H), 1.25 (s, 6H), 1.14-1.09 (m, 36H). ^{13}C NMR (126 MHz, $CDCl_3$): δ 139.81, 125.14, 103.02, 90.20, 81.60, 18.58, 11.32.

5. Supporting Figures and Tables

NMR Spectra

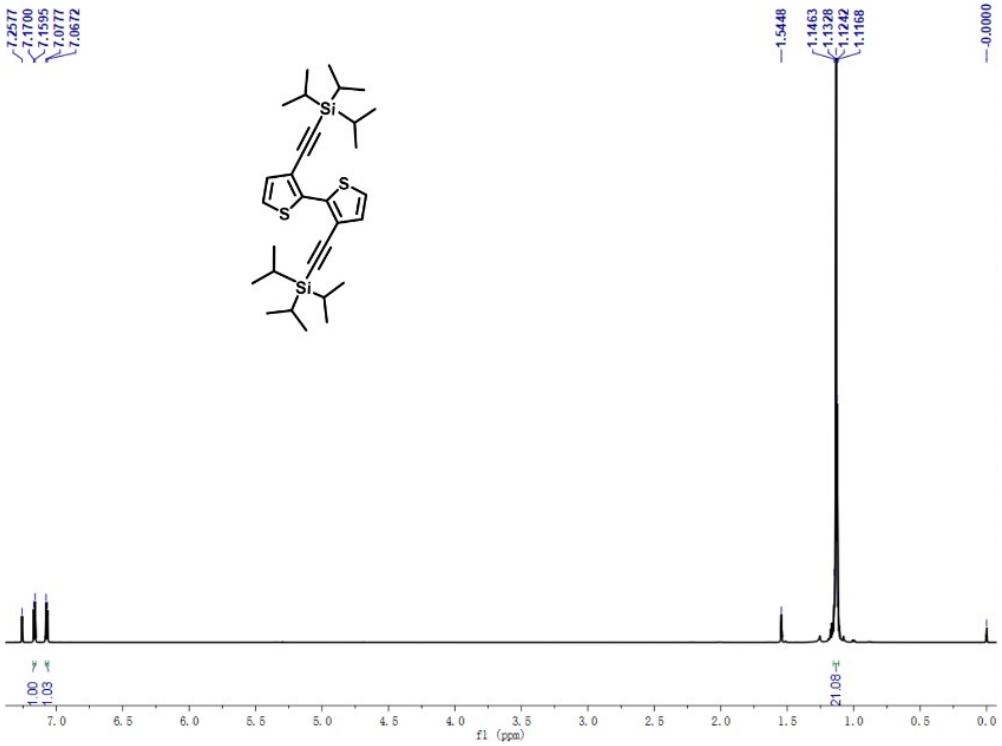

Fig. S1 ^{1}H NMR spectrum of **2T-Si** at 293K in $CDCl_3$.

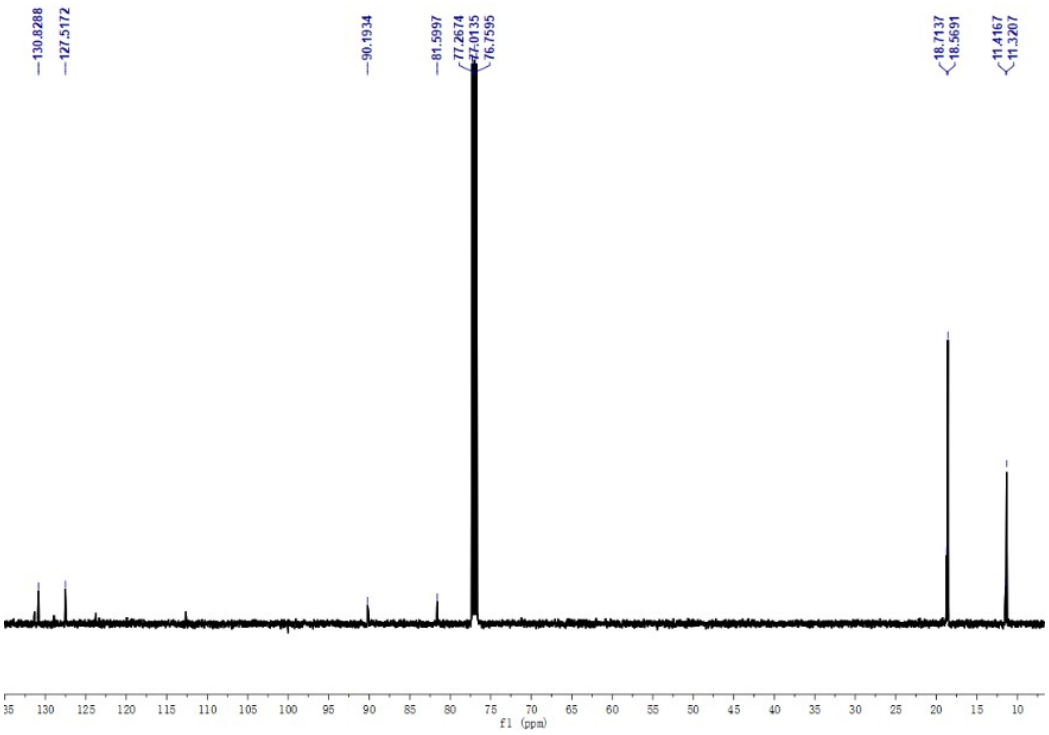

Fig. S2 ^{13}C NMR spectrum of **2T-Si** at 293K in $CDCl_3$.

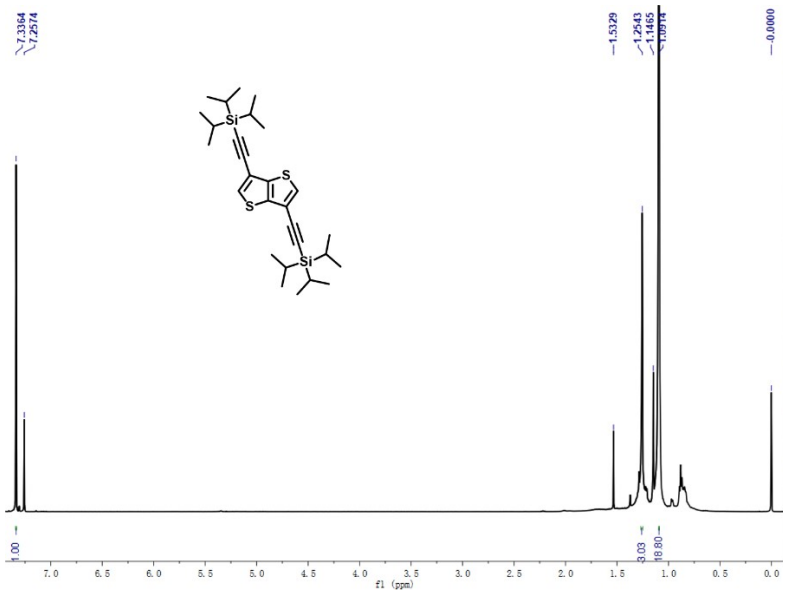

Fig. S3 ^{1}H NMR spectrum of **TT-Si** at 293K in $CDCl_3$.

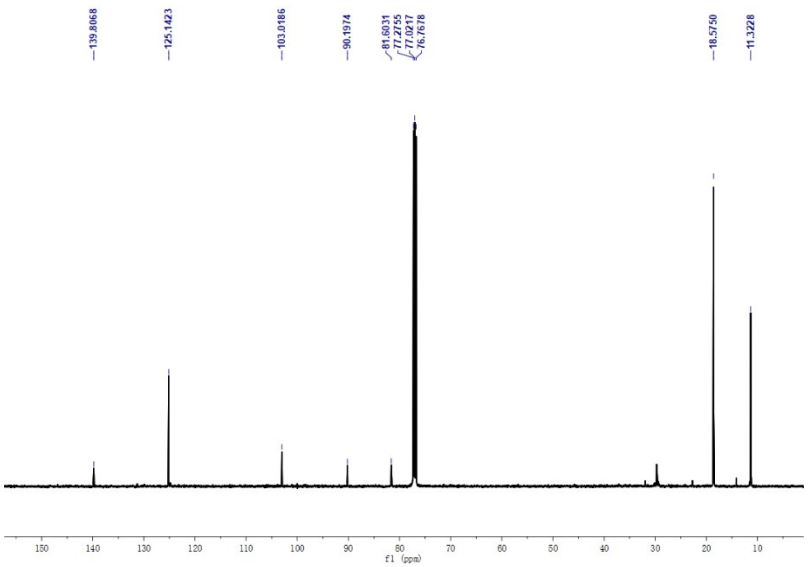

Fig. S4 ^{13}C NMR spectrum of **TT-Si** at 293K in $CDCl_3$.

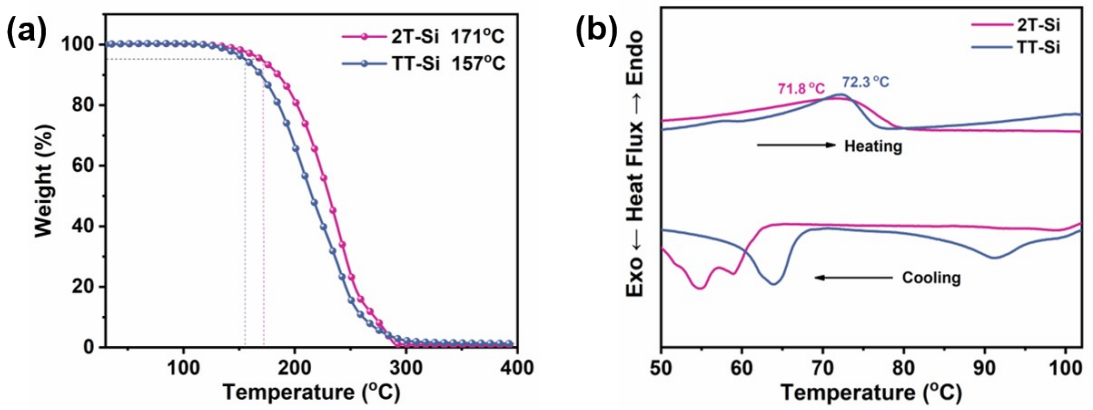

Fig. S5 (a) TGA curves and (b) DSC plots of 2T-Si and TT-Si.

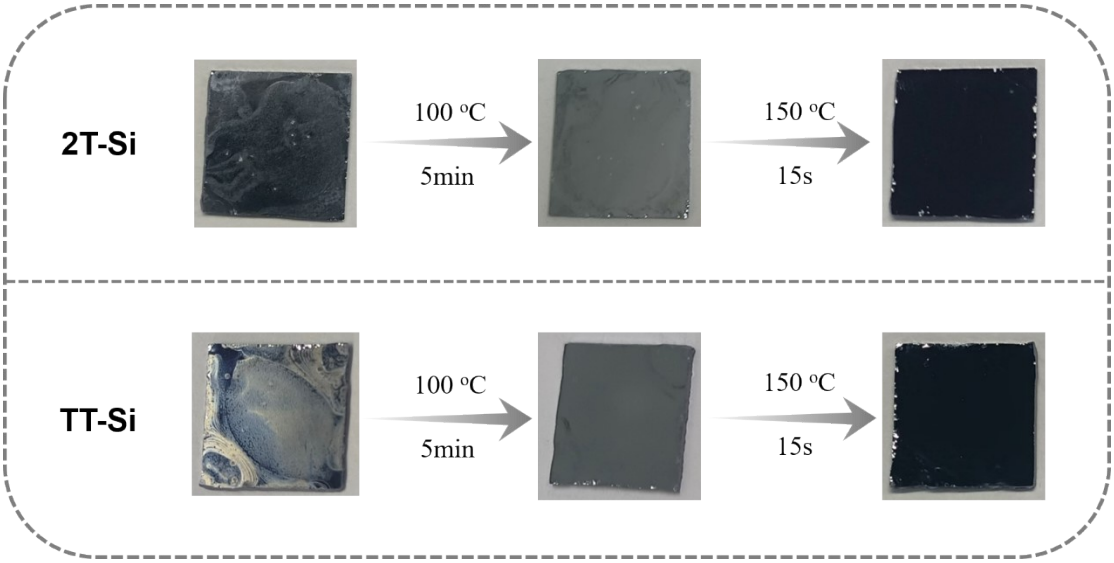

Fig. S6 Evolution of the pure additives film deposited on the silicon substrate in ambient.

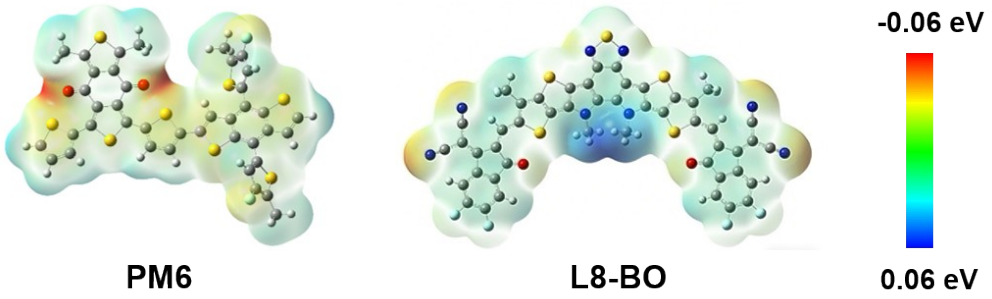

Fig. S7 Calculated ESP distribution of PM6 and L8-BO.

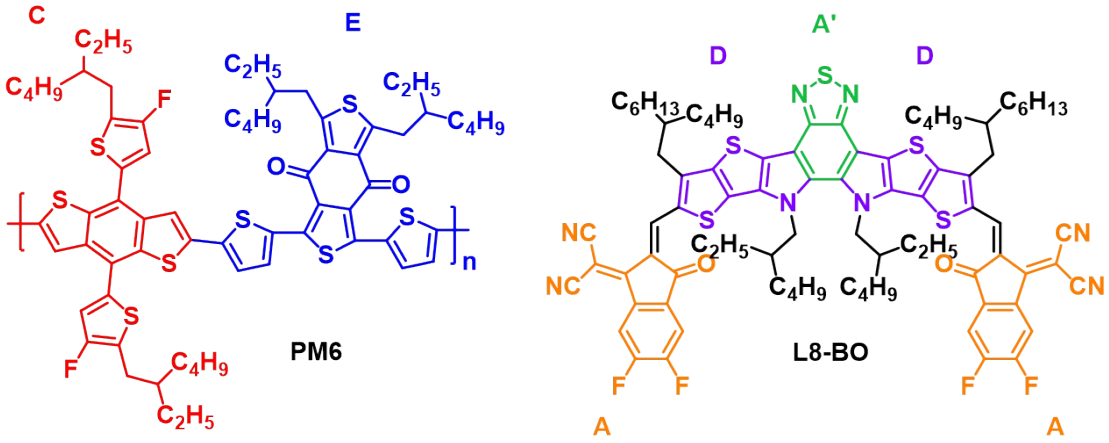

Fig. S8 Among PM6, the repeating unit of BDT-F in PM6 defined as C and the repeating unit of BDD in PM6 defined as E. Among chemical structures of L8-BO, the accepter-strong electron end group in NFA defined as A, the donor-strong electron group in NFA defined as D and the central accepter unit was defined as A'.

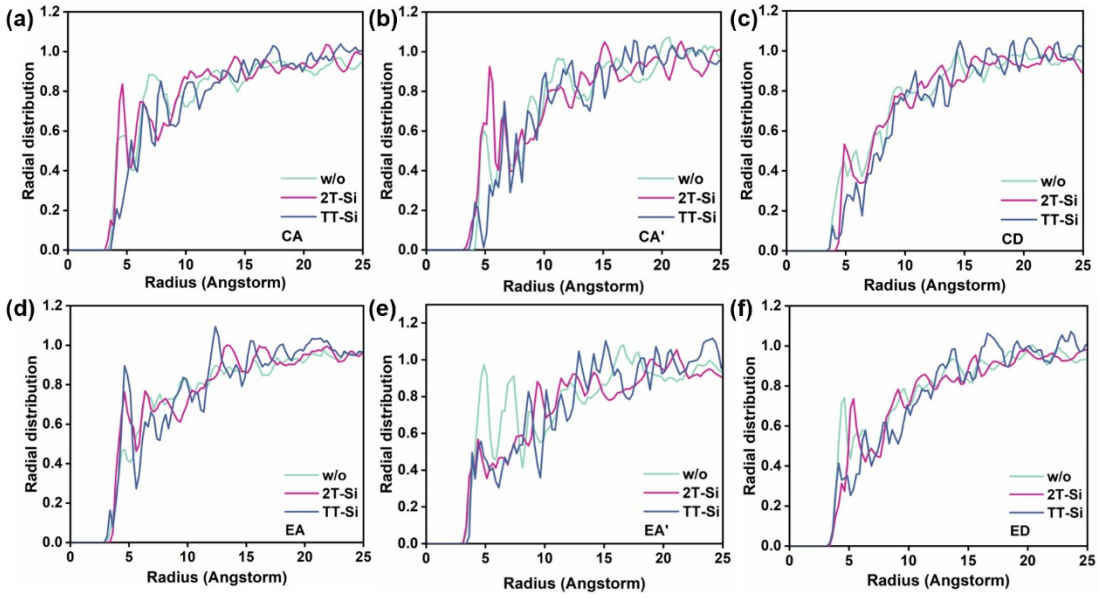

Fig. S9 Radial distribution function g (r) for the molecular fragments of PM6 and L8-

BO defined in Fig. S3 extracted from simulated blends.

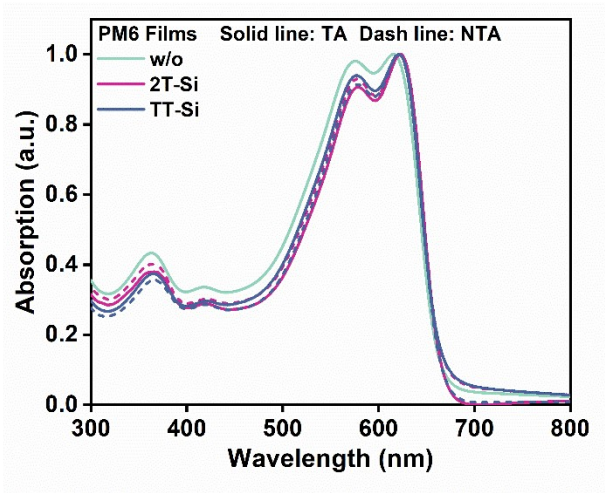

Fig. S10 Normalized absorption spectra of PM6 films with or without thermal annealing treatment.

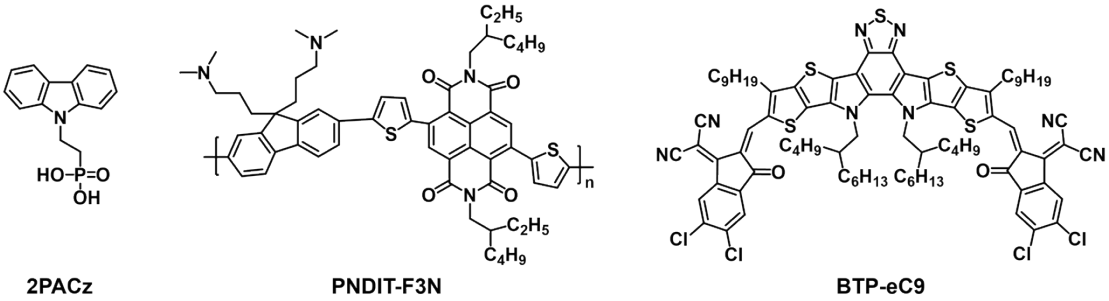

Fig. S11 Chemical structures of 2PACz, PNDIT-F3N and BTP-eC9.

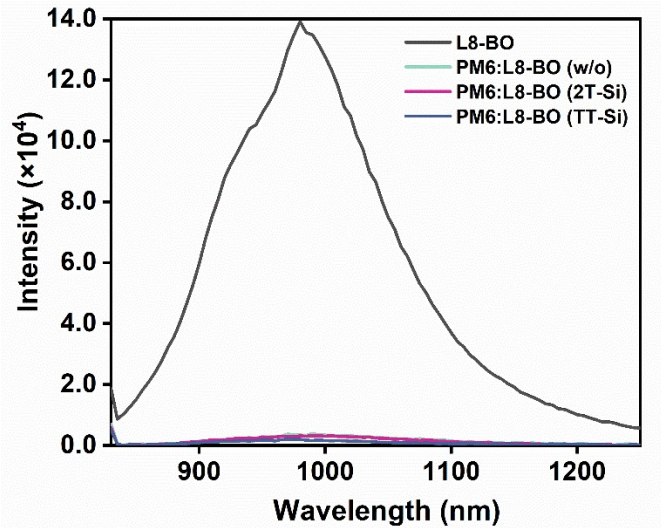

Fig. S12 PL spectra of the neat L8-BO film and the PM6:L8-BO film processed with

and without additives with the excitation wavelength at 800 nm

.

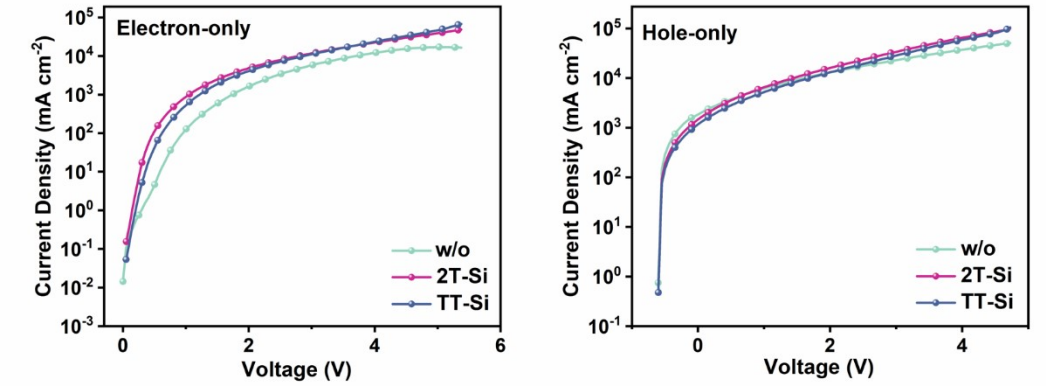

Fig. S13 The electron and hole mobility curves of additive-free and 2T-Si/TT-Si-treated PM6:L8-BO blend films.

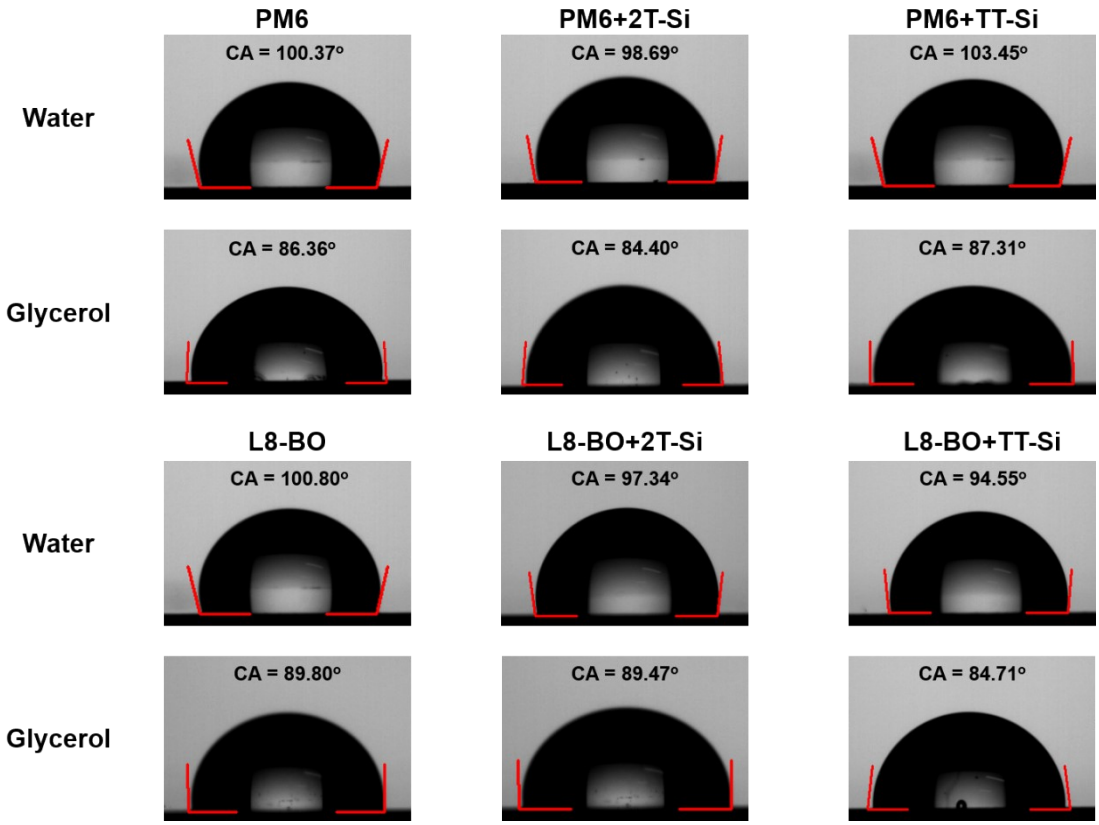

Fig. S14 Contact angle images of water and glycerol droplets on the surfaces of PM 6 and L8-BO films treated without/with different additives.

Table S1 Energy analysis of the interactions between solid additives and active materials.

Treatment	Interaction	PM6 (KJ/mol)	L8-BO (KJ/mol)
2T-Si	Electrostatic	-291.742	-458.013
	Van der Waals	-28688.6	-37772.9
	total	-28980.342	-38230.913
TT-Si	Electrostatic	-134.347	-285.489
	Van der Waals	-15945.8	-21117.3
	total	-16080.157	-21402.789

Table S2 Device parameters of PM6:L8-BO-based OSCs with different contents of 2T-Si.

Conditions	V_{oc} (V)	J_{sc} (mA cm^{-2})	J_{sc}^{cal} (mA cm^{-2})	FF (%)	PCE (%)
0	0.893	26.21	25.37	77.0	18.02
5%	0.900	26.03	24.70	79.3	18.57
10%	0.903	25.83	24.78	81.0	18.93
15%	0.890	26.62	25.51	79.5	18.83
30%	0.895	26.24	25.46	80.6	18.94
50%	0.882	27.28	26.55	80.04	19.26
70%	0.880	25.96	25.24	80.5	18.42

Table S3 Device parameters of PM6:L8-BO-based OSCs with different contents of TT-Si.

Conditions	V_{oc} (V)	J_{sc} (mA cm^{-2})	J_{sc}^{cal} (mA cm^{-2})	FF (%)	PCE (%)
0	0.893	26.21	25.37	77.0	18.02
10%	0.896	25.82	24.83	81.1	18.80
20%	0.881	27.23	26.04	79.1	19.00
30%	0.881	25.81	25.29	80.5	18.32
50%	0.882	26.31	25.45	80.4	18.67
70%	0.881	26.28	25.60	80.3	18.60

Table S4 Photovoltaic parameters of devices based on PM6:L8-BO with the recently reported solid additives and the halogenated analogues mentioned in the introduction.

Treatment	V_{oc} (V)	J_{sc} (mA cm^{-2})	FF (%)	PCE (%)	Ref.
FL	0.885	26.64	76.80	18.10	*Small*, 2024, **20**, 2405573.
DBT	0.877	26.52	75.84	17.63	
DBF	0.893	27.01	77.36	18.62	
TZ-Cl	0.899	26.71	76.31	18.30	*Energ. Environ. Sci.*, 2025, **18**, 2298-2307.
TZ-2Cl	0.901	27.01	75.93	18.50	
TZ-3Cl	0.903	27.29	80.19	19.80	
DTP	0.870	26.42	77.99	17.92	*Adv. Funct. Mater.*, 2024, **34**, 2401823.
DTH	0.861	27.07	79.40	18.51	
DTN	0.848	27.24	78.73	18.18	
SA-T5	0.879	26.65	80.30	18.80	*Nano Energy*, 2024, **125**, 109604.
2,2-TT	0.895	26.49	79.32	18.80	*Angew. Chem. Int. Edit.*, 2025, **64**, e202514004
2,3-TT	0.913	26.54	79.33	19.22	
3,3-TT	0.916	26.52	79.61	19.34	
3,6TTBr	0.890	26.80	80.40	19.10	*Adv. Mater.*, 2025, **37**, 2418393.
D1-H	0.867	26.71	76.10	17.62	*Adv. Funct. Mater.*, 2024, **35**, 2415090
D1-F	0.873	26.76	75.90	17.73	
D1-Cl	0.886	26.62	78.80	18.59	
TCBB-1	0.892	27.03	78.50	18.93	*J. Mater. Chem. A*, 2025, **13**, 35329-35341.
TCBB-2	0.882	26.20	77.95	18.01	
DBB	0.894	25.90	78.5	18.20	*Angew. Chem. Int. Edit.*, 2025, **64**, e202500085.
DFBB	0.898	26.40	80.8	19.20	
DBrTz	0.886	26.80	80.00	19.00	*Adv. Energy Mater.*, 2024, 2404507.
BrITz	0.886	26.30	78.30	18.20	
T3T	0.907	26.25	76.61	18.25	*Chem. Eng. J.*, 2025, **524**, 168963.
1-MN	0.883	26.82	77.22	18.29	*J. Mater. Chem. A*, 2025, **13**, 4600-4613.
2-MN	0.890	26.61	78.91	18.70	
2,7-MN	0.882	26.09	76.20	17.55	
2T-Si	0.882	27.28	80.04	19.26	This work
TT-Si	0.881	27.23	79.12	19.00	This work

Table S5 Photovoltaic performance parameters for the PM6:Y6, PM6:BO-4Cl and PM6:BTP-eC9 systems with and without 2T-Si as additive.

Active layers	Treatment	V_{oc} (V)	J_{sc} (mA cm^{-2})	FF (%)	PCE (%)
PM6:Y6	w/o	0.849	26.27	76.81	17.13
	2T-Si	0.825	26.92	78.99	17.54
PM6:BO-4Cl	w/o	0.872	26.75	78.05	18.20
	2T-Si	0.849	28.04	77.95	18.56
PM6:BTP-eC9	w/o	0.865	26.50	74.64	17.12
	2T-Si	0.852	27.98	80.65	19.22

The device parameters were obtained from over 10 devices.

Table S6 Summary of the GIWAXS parameters for the additive-free or 2T-Si/TT-Si-treated PM6, L8-BO, and PM6:L8-BO films.

Conditions	In-Plane Lamellar stacking				Out-of-Plane π-π stacking			
	q (Å^{-1})	d-spacing (Å)	FWHM (Å^{-1})	CCL (Å)	q (Å^{-1})	d-spacing (Å)	FWHM (Å^{-1})	CCL (Å)
PM6 (w/o)	0.27	22.11	0.11	56.52	1.56	4.02	1.23	4.59
PM6+2T-Si	0.29	21.88	0.08	70.69	1.58	3.97	0.51	11.08
PM6+TT-Si	0.28	22.03	0.09	62.37	1.58	3.97	0.66	8.56
L8-BO (w/o)					1.70	3.69	0.76	10.87
L8-BO+2T-Si					1.72	3.64	0.17	33.24
L8-BO+TT-Si					1.71	3.67	0.40	14.02
Blend (w/o)	0.29	21.65	0.16	35.34	1.65	3.80	0.433	13.05
Blend+2T-Si	0.30	20.93	0.10	56.55	1.69	3.73	0.334	16.92
Blend+TT-Si	0.30	20.93	0.12	47.12	1.66	3.78	0.403	14.02

Table S7 Fitting parameters of pristine and additive-processed films, where ξ, $2R_g$, and *D* are obtained from GISAXS fitting.

Active Layer	ξ (nm)	η (nm)	*D*	$2R_g$ (nm)
PM6:L8-BO (w/o)	21.8	6.3	2.2	23.6
PM6:L8-BO (2T-Si)	23.5	6.8	2.4	27.5
PM6:L8-BO (TT-Si)	22.3	6.5	2.4	26.3

Table S8 Parameters of contact angles and surface energies of films.

Treatment	Film	Contact angle [°]		γ	χ^{D-A}
		Water	Glycerine	(mN m^{-1})	(K)
w/o	PM6	100.37	86.36	24.31	0.32
	L8-BO	100.80	89.80	19.05	
2T-Si	PM6	98.69	84.40	25.68	0.98
	L8-BO	97.34	89.47	16.68	
TT-Si	PM6	103.45	87.31	27.60	0.54
	L8-BO	94.55	84.71	20.39	

References

1. M. J. Abraham, T. Murtola, R. Schulz, S. Páll, J. C. Smith, B. Hess and E. Lindahl, *SoftwareX*, 2015, **1-2**, 19-25.

2. B. Hess, H. Bekker, H. J. C. Berendsen and J. G. E. M. Fraaije, *J. Comput. Chem.*, 1997, **18**, 1463-1472.

3. M. Parrinello and A. Rahman, *J. Appl. Phys.*, 1981, **52**, 7182-7190.

4. S. Nosé, *J. Chem. Phys.*, 1984, **81**, 511-519.

5. A. D. W. Humphrey, K. Schulten., *J. Mol. Graph*., 1996, *14*.

6. S. Nilsson, A. Bernasik, A. Budkowski, E. Moons, *Macromolecules* 2007, **40**, 8291.

7. D. K. Owens, R. C. Wendt, *J. Appl. Polym. Sci.*, 1969, **13**, 1741.